Application of a novel method to identify multi-axis joint properties

Scott Noll, Jason Dreyer, and Rajendra Singh

The Ohio State University, 219 W. 19th Avenue, Columbus, Ohio 43210 USA

ABSTRACT

This article is motivated by the widespread use of shaped elastomeric body mounts that undergo broadband, multi-axis loading; whereas often in application, the principal direction mount properties are measured separately at single frequencies. An inverse method is applied to a new experiment that is constructed with an elastic metal beam end-supported by two elastomeric mounts. Due to a judiciously selected attachment location relative to the neutral axis of the beam as well as the shape of the mount, the in-plane transverse and longitudinal beam motions are found to be coupled. This method utilizes the sensitivity of the beam modal parameters, including natural frequency, mode shapes, and damping ratio, to support properties at each end to identify the multi-axis mount properties. The dynamic stiffness and loss factors of the elastomeric mounts are directly measured in a commercial elastomer test machine and agreement is found between the inverse and direct methods at small displacements. Further, this article helps provide insight into multi-axis properties with new benchmark experiments on off-the-shelf mounts that permit comparison between inverse system and direct component identification methods of the dynamic multi-axis elastomeric mount properties.

Keywords: Joint identification, Experimental dynamics, Stiffness coupling, Elastomer properties, Beam structures

INTRODUCTION

Elastomeric joints are widely used in vehicle isolation systems and their geometries are shaped to provide favorable properties in certain directions based on the diagonal terms [1, 2]. Nonetheless, non-diagonal (coupling) terms are often unknown though they are intrinsic to the design of complex automotive assemblies [3, 4]. Elastomeric joints present many challenges in modeling such as amplitude and frequency dependent properties. Direct measurement of the multidimensional dynamic properties of practical elastomeric joints is not possible, and these properties are further complicated when an elastomeric component is integrated into a sub-system assembly. Typically, the dynamic properties of assemblies may differ from those of components due to preload and boundary condition effects; therefore, there is a need to develop improved experimental methods to examine these issues [4]. Identification methods that utilize computational and experimental modal analyses may be integrated into some applications as long as the structures behave in a linear manner [5, 6]. For instance, Kim et al. [7] used a modal-based technique to characterize the dynamic stiffness of beam supports, each modeled by a lumped transverse spring. This prior method [7] has recently been extended by Noll et al. [8] to include the identification of multidimensional matrices. The method uses the physical system matrices developed from a discretized model (lumped parameter or finite element) without joints, and then measured natural frequencies, modal loss factors, and mode shapes are utilized to extract the joint parameters. This article provides an overview of an inverse identification method proposed recently by the same authors [8] and compares the results with the dynamic stiffness properties measured using a conventional direct test method.

PROBLEM FORMULATION

The scope of the inverse test is limited to an elastic beam structure connected to ground through two elastomeric joints, where each joint is comprised of two "off-the-shelf" mounts. The assembled system is assumed to be linear time invariant and self-adjoint; the damping of the elastomeric joints is structural, and the beam is assumed to be proportionally viscous damped. Further, the joint mass is known *a priori*, and the dynamic properties of a joint can be represented at a point by structural damping **h** and stiffness **k** matrices. The specific objectives of this article are as follows. 1. Design a tractable inverse beam experiment that allows a comparison with the direct measurement of the elastomeric component. 2. Use a recently extended inverse formulation of the authors [8] to identify fully populated joint dynamic matrices given limited modal measurements on the beam mount system. 3. Compare the dynamic joint properties identified with inverse and direct test methods.

The experiments are illustrated in Fig. 1; elastomeric mounts (Fig. 1a) are characterized in a single direction in a direct test method; An elastic beam system is supported by the same elastomeric mounts at each end offset from the neutral axis of the beam allowing for multi-axis loading. The offset attachment of the mounts introductes kinematic coupling to the structure which couples the slope $\theta(x,t)$ and longitudinal $u(x,t)$ motions of the beam. The modal parameters of the unconstrained (free-free) beam are selected so that the first elastic flexural mode is representative of the first elastic mode of real-world automotive subframe structures, say between 100 to 200 Hz. Further, the first 3 rigid body and 3 elastic modes (up to 1024 Hz) are examined, as both rigid and elastic modes are of concern in practical assemblies. Elastomeric mounts are intentionally selected even though they exhibit excitation amplitude and frequency dependent properties, as well as sample to sample variations (say about 10 to 15%).

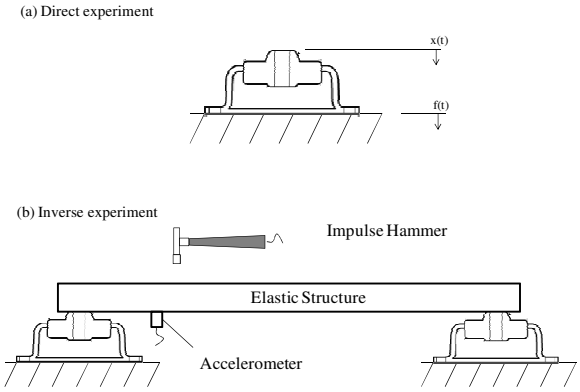

Fig. 1 Schematic of the direct and inverse experiments: (a) elastomeric mount loaded in compression and excited by a displacement input; (b) elastic beam is end supported by two mounts, where each is bolted to the beam; it is excited by an impulse hammer.

DIRECT JOINT IDENTIFICATION

The direct test employs a uniaxial hydraulically actuated, close loop servo-controlled elastomer test machine. A sinusoidal displacement, $x(t)$, is applied to the top side of the specimen, and the transmitted force, $f(t)$, at the bottom of the specimen is measured at the same frequency. The dynamic stiffness under a specified mean load is defined as $\tilde{k}_d(\omega) = \frac{f}{x} e^{i\delta} = \left|\tilde{k}_d\right| \angle\delta = k + ih = k(1 + i\gamma)$, where δ is the loss angle and $\gamma = \tan\delta$ is the loss factor. The elastomeric mount is characterized in a single direction as depicted in Fig 1a at an initial preset of 0.5 mm from 5 to 200 Hz at 5 Hz increments. The peak-to-peak amplitude is specified at 0.1 mm, 0.05 mm, or 0.01 mm.

INVERSE JOINT IDENTIFICATION

The multidimensional properties of the mounts are inversely identified from the experiment depicted in Fig. 1b including both stiffness and structural damping. The methodology combines experimental and modeling information in order to extract the joint properties. The flow-chart of the method is depicted in Fig. 2 that conceptually displays the procedure from an applications viewpoint. Rigorous mathematical details given in the article by Noll et al. [8]. The parameters of the inverse beam experiment are chosen in the context of automotive structural applications. The elastomeric mounts are selected to have similar stiffness properties to automotive bushings as well as the ratio of joint to structure stiffness. To maintain the lumped joint stiffness assumption, the ratio of the contact surface dimension to beam length is kept below 0.05. With these guidelines, a steel beam (with Young's modulus, E=207 GPa, Poisson's ratio, ν = 0.3, and mass density, ρ =7850 kg m^{-3}) is selected. The beam is 914 mm in length (L) with a rectangular cross-section of 25.4 x 50.8 mm where the thickness is 25.4 mm in the y direction for the desired flexural stiffness in the experiment. The beam is supported near each end by elastomeric mounts. The elastic center of the mount is intentionally offset from the neutral axis of the beam to ensure participation of multi-axis loading of the mount.

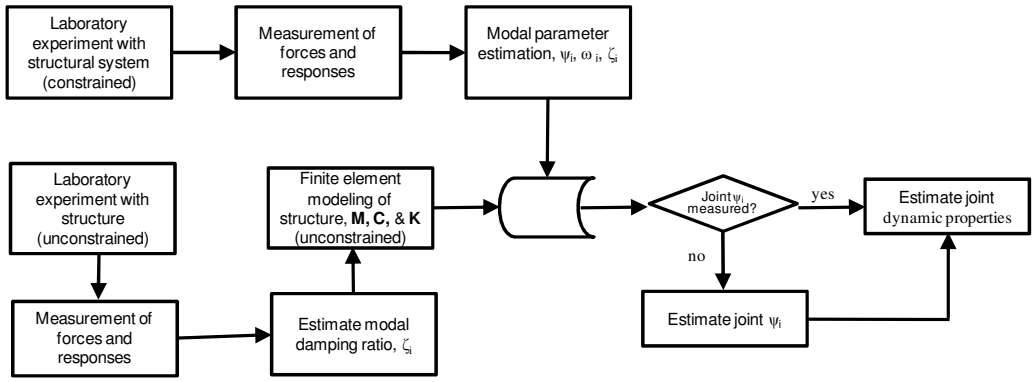

Fig.2 Flow-chart of the inverse joint identification method. Refer to Noll, et al. [8] for mathematical details.

The modal experiment is conducted for the inverse beam as depicted in Fig. 1 with the accelerometer positioned below point 3 (corresponds to node 3 of Fig. 2) and the roving impulse hammer technique is employed, with force inputs at points 1, 3-9, and 11 in the transverse direction and at points 1 and 11 in the longitudinal (x) direction. Ten impacts at each location are averaged to minimize random error in the accelerance $\widetilde{\boldsymbol{A}}_{ij}(\boldsymbol{\omega})$ measurements. For this work, a polyreference least-squares complex frequency-domain method is utilized where this implementation estimates the natural frequencies, damping parameters, and mode shapes in a global sense [6]. Although this measurement set results in mode shape estimates at each location, only the results near the joint locations are utilized in the identification procedure, e.g. at joint I, the mode shape components at points 1 and 3 are used. The mode shape components are averaged in the longitudinal (x) direction in both magnitude and phase.

COMPUTATIONAL MODEL

The computational model is comprised of 10 beam finite elements with lumped dynamic stiffness matrices at nodes 2 and 10 as depicted in Fig. 3. A two-node Timoshenko beam element is superposed with a longitudinal rod element to generate a two-node six degree of freedom element. This formulation assumes that elastic longitudinal and beam bending are uncoupled. The work of Friedman and Kosmatka [9] contains a complete derivation of the finite element stiffness and mass matrices for a Timoshenko beam. Each mount in the inverse experiment has a transverse eccentricity ε from the neutral axis of the beam from the beam's nodal coordinate system as shown in Fig. 3a. The eccentricity introduces a form of kinematic coupling that must be considered such that a suitable transformation can be made from the local coordinate system of the cylinder to the beam's nodal coordinate system. A mount exhibits a diagonal stiffness matrix at the component's elastic center as $\mathbf{k}_{mount} = diag\left[k_l \quad k_t \quad k_\theta\right](1+i\gamma)$, where k_t is the transverse stiffness, k_l is the longitudinal stiffness, and k_θ is the rotational stiffness. Assuming that the point stiffness at the elastic center follows a rigid connection to the beam neutral axis,

the effective stiffness matrix of the mount in the beam nodal coordinate system can be computed via the following transformation as

$$\mathbf{k}_{eff} = \mathbf{T}_\varepsilon \mathbf{k}_{mount} \mathbf{T}_\varepsilon^{-1} = \begin{bmatrix} k_l & 0 & \varepsilon k_l \\ 0 & k_t & 0 \\ \varepsilon k_l & 0 & k_\theta + \varepsilon^2 k_l \end{bmatrix} (1 + i\gamma); \quad \mathbf{T}_\varepsilon = \begin{bmatrix} 1 & 0 & 0 \\ 0 & 1 & 0 \\ -\varepsilon & 0 & 1 \end{bmatrix}. \tag{1}$$

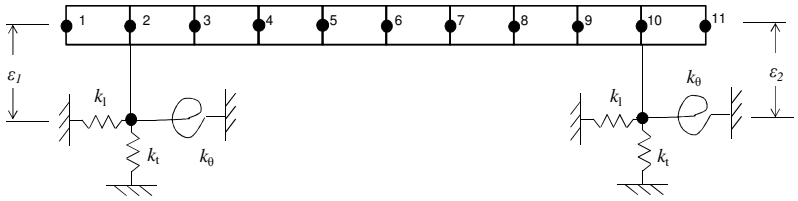

Fig. 3 Computational beam model with 10 elements and 11 nodes. Lumped stiffness elements are attached at nodes 2 and 10.

EXPERIMENTAL VALIDATION

After identification, the joint dynamic stiffness matrices are employed with the beam model to forward predict the natural frequencies and frequency response functions of the experiment. Table 1 lists the natural frequencies and the forward predictions which agree within 1% of the experimental results for six modes of vibration captured within the frequency range of 0-1024 Hz, including 3 rigid body and 3 elastic modes. Forward predictions of the accelerance spectra $\tilde{\mathbf{A}}(\omega)$ are computed by a direct inversion of the assembled dynamic stiffness matrices:

$$\tilde{\mathbf{A}}(\omega) = -\omega^2 (\mathbf{Z}(\omega) + \mathbf{z})^{-1} \mathbf{f}(\omega). \tag{2}$$

Table 1. Comparison of natural frequencies between the experiment and theory

Mode Index r	Experiment $\omega_r / 2\pi$ (Hz)	Theory $\omega_r / 2\pi$ (Hz)	Percent Difference
1	39.1	39.0	0.3%
2	59.2	59.3	-0.2%
3	69.4	69.1	0.4%
4	187	188	-0.5%
5	474	472	0.4%
6	916	914	0.2%

The driving point comparison in Fig. 4 exhibits good agreement, though some regions show discrepancies most notably at the anti-resonance near 400 Hz. The direct identification of the dynamic stiffness of the elastomeric mount exhibits considerable amplitude and frequency dependence as shown in Fig. 5. The highest sensitivity to frequency dependence is observed below 50 Hz. The loss factor (Fig. 5b) is nearly constant with respect to frequency above 50 Hz; however, it decreases by one-third when the peak-to-peak amplitude of the excitation is reduced from 0.1 mm to 0.01. A statistical analysis of the observations, curve-fitted values, and residuals is performed to establish a confidence interval for the identified stiffness matrix assuming a normal distribution and a confidence level of 95%. A comparison of the direct and inverse dynamic stiffness is shown in Fig. 5. Generally, there is good agreement between the inverse tests and the 0.01 mm peak-to-peak excitation amplitude.

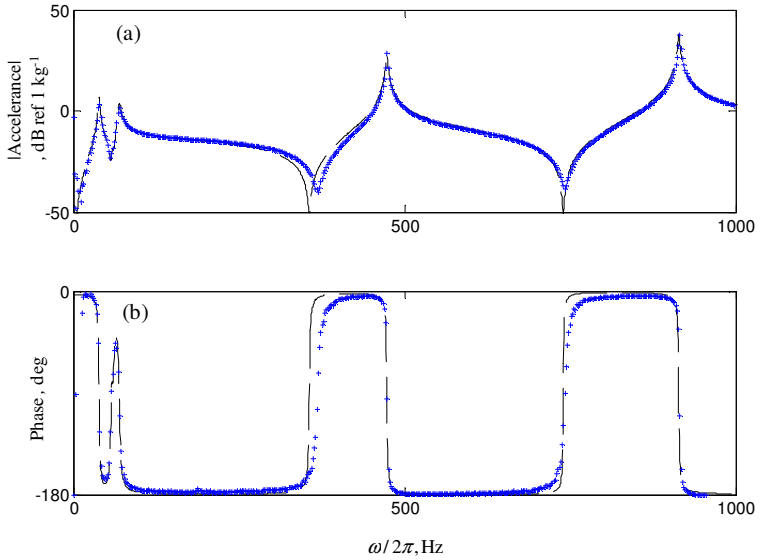

Fig. 4 Driving point accelerance for the resonant beam experiment in the transverse direction at point 3 as displayed in Fig. 3: (a) magnitude; (b) phase. Key: (—) predicted using Eqn. (2) ; (+) measured.

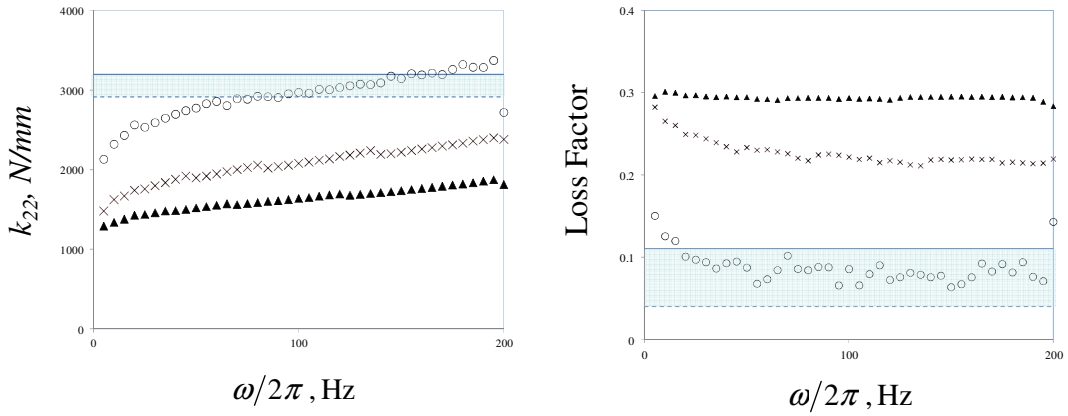

Fig. 6 Comparison of stiffness and loss factor identified through inverse and direct tests. key: direct test with pk-pk amplitude of ○ 0.01mm, x 0.05 mm, and ▲ 0.1 mm ; ------ inverse method with 95% confidence interval.

ESTIMATION OF THE MOUNT ELASTIC CENTER

The elastic center of the of each mount can be estimated from the inverse beam experiment by rearranging the k_{13} element of equation 3 and solving for ε as $\varepsilon = k_{13}/k_l$, where k_{13} and k_l are previously identified from the inverse experiment. For a comparison, a finite element model of the elastomeric mount is created. The purpose of this model is to locate the elastic center considering the unique geometry of the elastomeric mount and as such a number of simplifying assumptions are made. First, the elastomeric material is assumed to have no residual stress or strain. Second, at small displacements, the material can be represented as a linear elastic material with a poisson's ratio of 0.49 which approximates the nearly incompressible behavior of elastomers. Also, the housing of the mount is rigid in comparison to the elastomer and is modeled as a fixed boundary at the housing / elastomer interface. Finally, the vertical preload due to supporting the beam is not considered. The elastic center is then systematically investigated by applying a point force in the x-direction at varying offsets in the y-direction until no gross component rotational displacement, θ, is observed. Therefore, the computed ε is the sum of one-half the thickness of the beam in addition to the offset location found in the finite element study. Reasonable agreement is found between the identified and computed location of the elastic center and is illustrated in Table 2.

Table 2. Transverse eccentricity, ε

Method	ε, mm
Inverse, Eqn. 6, Joint I	34
Inverse, Eqn. 6, Joint II	20
Finite element model	26.7

CONCLUSION

This article has contributed to the state of the art by designing new experiments and methods that permit a direct comparison of inverse and direct methods including non-diagonal terms in the stiffness matrices of joints. The proposed methodology is employed to identify the dynamic stiffness properties of joints with dimension 3 in the inverse experiment consisting of an elastic beam with two elastomeric supporting elements. A forward model successfully predicts the measured modal parameters and accelerance spectra. Good agreement is found for dynamic stiffness and loss factors between the inverse and direct methods. The methods in this article are not limited to metal beam and elastomeric joint systems, but rather are applicable to a more general class of jointed assemblies. The inverse test in this article is limited to an examination of the linearized joint properties; however, the design lends itself well to incorporate different excitation levels to examine the amplitude-dependent properties of elastomers. Further, with two opposing joints, preload or displacement can be easily added without altering the system. Finally, the work has been limited to a single structure connected to ground, whereas many real-world assemblies contain two or more substructures. Despite these limitations, this article provides valuable insights for interpreting direct component test data with modal system data even when the selected elastomer exhibits strong amplitude dependent properties.

REFERENCES

1. C. Lewitzke and P. Lee, "Application of elastomeric components for noise and vibration isolation in the automotive industry", SAE Technical Paper 2001-01-1447 (2001).
2. H.Y. Oh and K.J. Kim, "Design of shape for visco-elastic isolation element by topological and shape optimization methods", SAE Technical Paper 2009-01-2127 (2009).
3. H.J. Kim and K.J. Kim, "Effects of rotational stiffness of bushings on natural frequency estimation for vehicles by substructure coupling based on frequency response functions", *Int. J. Vehicle Noise and Vib*. 6 (2010) 215-229.
4. S. Kim and R. Singh, "Multi-dimensional characterization of vibration isolators over a wide range of frequencies", *Journal of Sound Vibration*, 245 (2001) 877 – 913.
5. R.D. Cook, D.S. Malkus, and M.E. Plesha, *Concepts and applications of finite element analysis*, third edition, John Wiley & Sons, New York, 1989.
6. B. Peeters, H. Van der Auweraer, P. Guillaume, and J. Leuridan, "The PolyMAX frequency-domain method: a new standard for modal parameter estimation?" *Shock and Vibration,* 11 (2004) 395-409.
7. T.R. Kim, K.F. Ehmann, and S.M. Wu, "Identification of joint structural parameters between substructures," *J. Eng. Ind.*, 113 (1991) 419–424.
8. Noll, S., Dreyer, J., Singh, R., "Identification of dynamic stiffness matrices of elastomeric joints using direct and inverse methods," *Mechanical Systems and Signal Processing*, (2013), 39 (2013) 227-244, http://dx.doi.org/10.1016/j.ymssp.2013.02.003i.
9. Z. Friedman and J. Kosmatka, "An improved two-node Timoshenko beam finite element," *Computers and Structures*, 47 (1993) 473 – 481.

ACKNOWLEDGMENTS

We acknowledge the member organizations such as Transportation Research Center Inc., Honda R&D Americas, Inc., and F.tech of the Smart Vehicle Concepts Center (www.SmartVehicleCenter.org) and the National Science Foundation Industry/University Cooperative Research Centers program (www.nsf.gov/eng/iip/iucrc) for supporting this work.